Antisite defect-free $Lu_3(Ga_xAl_{1-x})_5O_{12}$:Pr scintillator

M. Nikl,[a] J. Pejchal, E. Mihokova, and J. A. Mares
Institute of Physics AS CR, Cukrovarnicka 10, 16253 Prague, Czech Republic

H. Ogino, A. Yoshikawa, and T. Fukuda
Institute of Multidisciplinary Research for Advanced Materials, Tohoku University, 2-1-1 Katahira, Aoba-ku, Sendai 980-8577, Japan

A. Vedda
Dipartimento dio Scienza dei Materiali dell' Università di Milano "Bicocca" and CNISM, Via Cozzi 53, 20 125 Milano, Italy

C. D'Ambrosio
CERN, PH-TA2 group, CH-1211, Geneve 23, Switzerland

(Received 29 November 2005; accepted 12 February 2006; published online 5 April 2006)

Pr-doped $Lu_3(Ga_xAl_{1-x})_5O_{12}$:Pr, $x=0-1$, single crystals were grown by the micro-pulling-down method. We study luminescence and scintillation characteristics of the sample set focusing on their dependence on the gallium content. For $x=0.4$ we obtain the high figure-of-merit material with elevated density, high efficiency, and very fast scintillation response below 20 ns without any slower components. Improvement of scintillation performance is explained as due to the absence of the antisite Lu_{Al} defects that was for the first time realized in such bulk garnet single crystals grown from the high temperature melt. © *2006 American Institute of Physics*. [DOI: 10.1063/1.2191741]

Research and development of high density, fast, and efficient scintillator materials within the last 10–15 years was mainly triggered by the need of modern imaging techniques in medicine, namely, the positron emission tomography (PET). The performance of PET was limited by the use of $Bi_4Ge_3O_{12}$ (BGO) scintillator. As a result, Ce-doped silicates, namely, the Gd_2SiO_5 (GSO), Lu_2SiO_5 (LSO), and most recently $(Lu_{1-x}Y_x)_2SiO_5$ (LYSO) single crystal hosts (see Refs. 1–3) were developed. A need for another scintillator material with similar performance appeared due to considered depth-of-interaction problem in PET,[4] since the usage of two somewhat different materials in a suitable detector geometry can further enhance the precision of space resolution in three-dimensional (3D) imaging in PET method. Ce-doped perovskite $LuAlO_3$ (LuAP) or $(Lu_{1-x}Y_x)AlO_3$ (LuYAP) single crystals have been considered and widely studied candidates for this purpose (see Ref. 5 for a review). As reported recently,[6] the latter is reaching the prototype industrial production stage. However, with respect to YAP:Ce, Lu-rich perovskites show the light yield lower by a factor of 1.5–2 and their scintillation decay contain intense and noticeably slower component. Apart from perovskites, Ce-doped $Lu_3Al_5O_{12}$ (LuAG) single crystals with very similar figure of merit in comparison with GSO:Ce scintillator were reported in the literature.[7,8] After a few introductory studies in the 1990s (Ref. 9) a renewed interest in the Pr^{3+} doping of some of the hosts above mentioned appeared recently. Namely, the Pr-doped yttrium aluminum garnet (YAG),[10] LuAG,[11] LuAP,[12] and LSO[13,14] single crystals have been reported and especially the LuAG host appeared interesting because of absence of the $5d-4f$ emission quenching and/or ionization of the $5d_1$ state at room temperature.[15] It is well known, however, that temporal characteristics in aluminum garnet-based fast scintillators are degraded due to the occurrence of the antisite defects (Y or Lu ions at the octahedral *Al* site).[16] Recently, electron traps associated with such defects were identified in LuAG:Ce (Ref. 17) with the help of thermoluminescence measurements. Enhanced retrapping of migrating electrons at such shallow traps before their radiative recombination with holes at the Ce^{3+} centers results in very slow scintillation decay components that are technically unexploitable. Consequently, the light yield and scintillation response of such material are degraded.[18] While antisite defect-free thin films of Ce-doped YAG or LuAG scintillators prepared from a flux by the liquid phase epitaxy method were reported,[19] so far no such achievement was accomplished in the bulk crystal prepared from the high temperature melt.

The aim of this letter is to present an antisite defect-free Pr-doped garnet scintillator. Admixture of Ga^{3+} ions in the Lu garnet host structure remarkably reduced the above mentioned antisite defect-associated electron traps. As a result, an energy transfer to Pr^{3+} centers was significantly accelerated. We study the optical and scintillator characteristics and we discuss the figure of merit of such new bulky scintillator.

The single crystals of $Lu_3(Ga_xAl_{1-x})_5O_{12}$, $x=0-1$, doped by Pr^{3+} (0.3%–1% in the melt) were grown by the micro-pulling-down technique, the details will be published elsewhere. Crackless, transparent, a few centimeter long rods with a diameter of about 4 mm were obtained. Plates of dimensions about $3.5\times8\times1$ mm^3 were cut and polished for the experiments. Absorption spectra were measured by UV/Vis/NIR Shimadzu absorption spectrometer UV-3101PC. Radioluminescence (RL) spectra and scintillation decays were measured with a modified Spectrofluorometer 199S, Edinburgh Instrument, using excitation by an x-ray tube and ^{22}Na radioisotope, respectively. Emission spectra were corrected for experimental distortions and true decay times were extracted from the decay curves using a deconvolution procedure (SpectraSolve software of LASTEK Ltd.). Wavelength-resolved thermally stimulated luminescence (TSL) measurements were performed in the 10–310 K range after x-ray irradiation at 10 K (by a Philips 2274 x-ray tube operated at 20 kV), with a homemade apparatus allowing the

[a]Electronic mail: nikl@fzu.cz

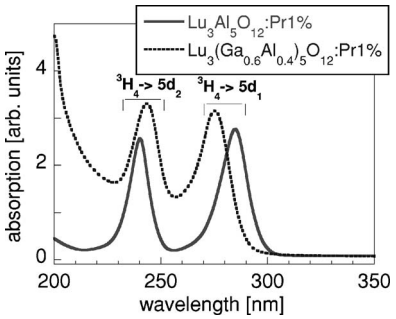

FIG. 1. Absorption spectra of Pr-doped garnets at room temperature. Composition is given in the legend.

detection of the TSL signal both as a function of temperature and wavelength in the 280–710 nm interval. Light yield (LY) was measured by a hybrid photomultiplier tube (HPMT)-based detector using 662 keV line of ^{137}Cs radioisotope (for other experimental details see Refs. 7, 8, 11, and 14).

Absorption spectra of the samples for $x=0$ and $x=0.6$ are given in Fig. 1. The observed absorption bands in the ultraviolet (UV) spectral range can be ascribed to the absorption transitions to the $5d_1$ and $5d_2$ states in agreement with Ref. 11. It is worth noting that the admixture of Ga^{3+} results in high-energy shift of the $5d_1$ band and lesser energy separation between $5d_1$ and $5d_2$ bands. Such a tendency can be explained by the decrease of both the crystalline field at the Lu^{3+} site and its interaction with the lattice due to increased covalent bonding between the Ga^{3+} and O^{2-} ions in the lattice, which effectively takes further away O^{2-} outer electrons around the Lu^{3+} lattice site [see the sketch of yttrium gallium garnet (YGG) structure in Ref. 20].

Radioluminescence spectra for $x=0$, 0.4, 0.6, and 1.0 are given in Fig. 2 in an absolute comparison with the BGO standard sample of the same shape. With increasing Ga content the emission intensity decreases in a similar manner as observed for Pr^{3+}-doped YAG-YGG ceramic samples.[21] It is interesting to note that emission lines belonging to the $4f-4f$ transitions of Pr^{3+} are getting stronger with increasing Ga content, which point to a different mechanism of the corresponding level population and interaction with the surroundings with respect to $5d_1$ level. Increased value of Stokes shift was noticed: while in LuAG:Pr it is about 0.35 eV, in $Lu_3(Ga_{0.6}Al_{0.4})_5O_{12}$:Pr it exceeds 0.40 eV. Increased Stokes shift decreases reabsorption losses in bulky scintillator segments.

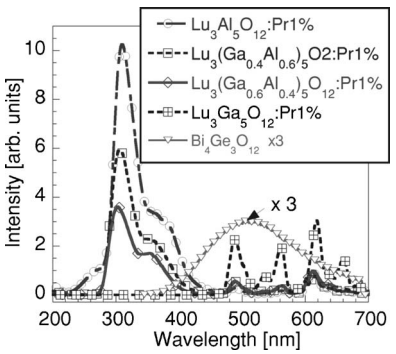

FIG. 2. Radioluminescence spectra of Pr-doped garnets at room temperature (x-ray tube, 35 kV). Spectra are mutually comparable in an absolute scale and are compared also to a BGO reference sample.

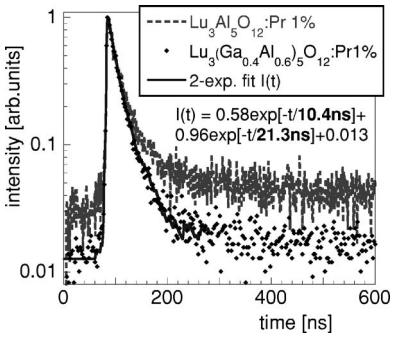

FIG. 3. Spectrally unresolved normalized scintillation decay curves measured in the same conditions at room temperature. The decay of $Lu_3Ga_2Al_3O_{12}$:Pr1% is approximated by the function $I(t)$ displayed in the figure. The fit is given by a solid line, obtained by convolution of the instrumental response (not in the figure) and the function $I(t)$.

The acceleration of the scintillation decay curve within the first 100 ns was observed with increasing Ga concentration in a very similar manner as in photoluminescence decays for the same samples. Moreover, an increased ratio between the decay amplitude and signal level before the rising edge of the decay curve was obtained, see Fig. 3. The latter tendency can be explained as due to the decreased retrapping of charge carriers during their migration and consequently faster energy transfer from the host lattice to Pr^{3+} ions, see also Ref. 18. Acceleration of the decay curve within the first 100 ns in both photoluminescence and scintillation decay can be explained by a nonradiative transfer of electron away from the $5d_1$ relaxed excited state. Two mechanisms can be considered: (i) due to enhanced ability of Ga^{3+} ions to capture electron, there can be an electron transfer from $5d_1$ level towards Ga^{3+} followed by nonradiative relaxation of created $Pr^{4+}-Ga^{2+}$ complex back to the ground state of the lattice. Such processes were considered, e.g., in CeF_3, see Ref. 5 for the review; (ii) Ga^{3+} wave functions will lower the edge of the conduction band[22] and allow for the ionization of relaxed $5d_1$ level, i.e., an escape of electron to the conduction band.

Light yield was measured under 662 keV excitation for several $Lu_3(Ga_{0.4}Al_{0.6})_5O_{12}$:Pr samples within the 500 and 1000 ns time gate using HPMT detector and compared with that of BGO measured with the latter gate. Values of light yield between 110% and 160% of (spectrally corrected) BGO were evaluated from the energy spectra and position of the photopeak. There is no difference in the values obtained within the 500 and 1000 ns time gate, which also confirms the absence of slower decay components.

To further verify the situation regarding shallow trapping states in these samples, thermoluminescence glow curves and spectra were measured after x-ray irradiation at 10 K (see Fig. 4) for $Lu_3Al_5O_{12}$:Pr and $Lu_3(Ga_{0.4}Al_{0.6})_5O_{12}$:Pr samples, and compared with high quality Czochralski-grown $Lu_3Al_5O_{12}$:Ce single crystal with similar Ce concentration in the crystal, see also Ref. 17. While below 260 K TSL glow curves for the Ce^{3+} and Pr^{3+}-doped LuAG host crystal appear rather similar, their TSL emission spectra are completely different (see the inset of Fig. 4) and coincide with luminescence characteristics of Ce^{3+} and Pr^{3+} ions, respectively. Such result can be explained as that TSL glow curves are determined by the same electron traps in both samples, while holes are captured at the Ce^{3+} or Pr^{3+} ions. Liberation of electrons from traps and their recombination with temporary Ce^{4+} or Pr^{4+} hole centers is then obtained in the TSL run and

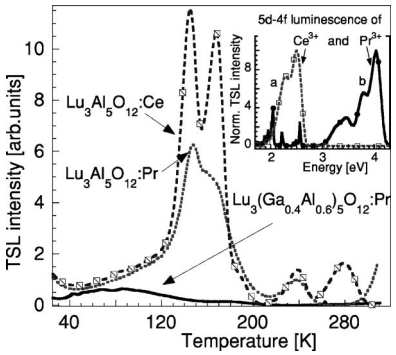

FIG. 4. Thermoluminescence glow curves after x-ray irradiation at 10 K. In the inset the TSL emission spectra within 120–180 K are given for $Lu_3Al_5O_{12}$:Ce (a) and $Lu_3Al_5O_{12}$:Pr (b) samples.

determine the glow curve and the shape of emission spectra. Similarity of glow curves within 120–200 K in both samples provides additional support for the conclusion of Ref. 17 that related electron traps are associated with the antisite Lu_{Al} defects as these defects are expected to occur in the same manner in both samples. However, striking reduction of TSL signal is obtained in the glow curves of $Lu_3(Ga_{0.4}Al_{0.6})_5O_{12}$:Pr sample, while emission spectrum is the same with respect to that already described LuAG:Pr. Complete disappearance of the glow curve structure within 120–200 K can be explained by the disappearance of antisite defects and is fully coherent with the speedup of the scintillation response described above. It is worth noting that in Ga-containing samples there is no shoulder in the radioluminescence spectra around 260–270 nm observed in the Ga-free sample, see Fig. 2. This shoulder belongs to the host emission ascribed to the exciton trapped around the antisite defect[23] or to the radiative recombination of an electron with the hole trapped around the antisite defect.[19] In either case this emission center includes the Lu_{A1} defect and its disappearance further supports the conclusion that these defects disappeared in the Al–Ga intermediate compositions.

There is no straightforward explanation of such efficient suppression of the Lu_{Al} antisite defects in the studied Pr-doped $Lu_3(Ga_xAl_{1-x})_5O_{12}$ (x=0.4–0.6) single crystals grown from the high temperature melt, because their concentration was found several times higher in $Y_3Ga_5O_{12}$ ($Lu_3Al_5O_{12}$) single crystals with respect to their aluminum counterparts.[24] It can be suggested that such effect arises due to the selective occupation of the *A*l sites by Ga ions in the mixed compositions. Namely, the ratio of ionic radiuses of the Ga^{3+} and Al^{3+} ions at the four- and six-coordinated sites is calculated as ~1.21 and ~1.15, respectively, which points to the preferential replacement/occupation of the octahedral *A*l sites by the Ga^{3+} ions. It can limit an incorporation of the Lu ions in the AlO_6 octahedra, and consequently the Lu_{Al} defect creation in such intermediate (x=0.4–0.6) compositions.

To summarize, the admixture of Ga^{3+} in LuAG:Pr scintillator enhances its scintillation performance even if the overall scintillation efficiency (radioluminescence intensity) with increasing concentration of Ga is gradually decreasing. Single crystal of $Lu_3(Ga_{0.4}Al_{0.6})_5O_{12}$:Pr has the density about 7.0 g/cm^3, emission maximum around 302 nm, scintillation $1/e$ decay time about 18 ns, there are no slower decay processes, and its light yield is between 110% and 160% of BGO. For the first time, in the melt-grown bulky gallium-aluminum garnet the antisite defects were suppressed and consequently the energy transfer from the host to the Pr^{3+} emission centers significantly accelerated. All these features characterize a scintillation material, in which 90% of the scintillation response is collected within the 100 ns time gate. This material appears a highly competitive candidate for becoming a partner of LYSO:Ce in the depth-of-interaction corrected PET machine.

Financial support of the Czech GA AV No. S100100506 and MSMT KONTAKT 1P2004ME716 projects together with Japanese Industrial Technology Research Grant Program in 03A26014a from New Energy and Industrial Technology Development Organization (NEDO) as well as Grant in Aid for Young Scientists (A), 15686001, 2003 by Ministry of Education, Culture, Sports, Science, and Technology of Japanese government (MEXT) are gratefully acknowledged.

[1] H. Ishibashi, K. Shimizu, K. Susa, and S. Kubota, IEEE Trans. Nucl. Sci. **36**, 170 (1989).
[2] H. Suzuki, T. A. Tombrello, C. L. Melcher, and J. S. Schweitzer, Nucl. Instrum. Methods Phys. Res. A **320**, 263 (1992).
[3] P. Szupryczynski, C. L. Melcher, M. A. Spurrier, M. P. Maskarinec, A. A. Carey, A. J. Wojtowicz, W. Drozdowski, D. Wisniewski, and R. Nutt, IEEE Trans. Nucl. Sci. **51**, 1103 (2004).
[4] T. F. Budinger, K. M. Brennan, W. W. Moses, and S. E. Derenzo, Nucl. Med. Biol. **23**, 659 (1996).
[5] M. Nikl, Phys. Status Solidi A **178**, 595 (2000).
[6] C. Kuntner, E. Auffray, D. Bellotto, C. Dujardin, N. Grumbach, I. A. Kamenskikh, P. Lecoq, H. Mojzisova, C. Pedrini, and M. Schneegans, Nucl. Instrum. Methods Phys. Res. A **537**, 295 (2005).
[7] M. Nikl, E. Mihokova, J. A. Mares, A. Vedda, M. Martini, K. Nejezchleb, and K. Blazek, Phys. Status Solidi B **181**, R10 (2000).
[8] J. A. Mares, A. Beitlerova, M. Nikl, N. Solovieva, C. D'Ambrosio, K. Blazek, P. Maly, K. Nejezchleb, and F. de Notaristefani, Radiat. Meas. **38**, 353 (2004).
[9] C. W. E. van Eijk, P. Dorenbos, and R. Visser, IEEE Trans. Nucl. Sci. **41**, 738 (1994).
[10] W. Drozdowski, T. Lukasiewicz, A. J. Wojtowicz, D. Wisniewski, and J. Kisielewski, J. Cryst. Growth **275**, e709 (2005).
[11] M. Nikl, H. Ogino, A. Krasnikov, A. Beitlerova, A. Yoshikawa, and T. Fukuda, Phys. Status Solidi A **202**, R4 (2005).
[12] W. Drozdowski, A. J. Wojtowicz, D. Wisniewski, T. Lukasiewicz, and J. Kisielewski, Opt. Mater. (Amsterdam, Neth.) **28**, 102 (2006).
[13] E. van der Kolk, P. Dorenbos, C. W. E. van Eijk, S. A. Basun, G. F. Imbusch, and W. M. Yen, Phys. Rev. B **71**, 165120 (2005).
[14] M. Nikl, H. Ogino, A. Yoshikawa, E. Mihokova, J. Pejchal, A. Beitlerova, A. Novoselov, and T. Fukuda, Chem. Phys. Lett. **410**, 218 (2005).
[15] M. Nikl, J. Pejchal, A. Yoshikawa, T. Fukuda, A. Krasnikov, A. Vedda, and K. Nejezchleb, *Proceedings of the 8th International Conference on Inorganic Scintillators*, Alushta, Ukraine, 19–23 September 2005 (ISC Kharkov, 2005); Functional Materials 2006.
[16] V. Lupei, G. Boulon, and A. Lupei, J. Phys.: Condens. Matter **5**, L35 (1993).
[17] M. Nikl, E. Mihokova, J. Pejchal, A. Vedda, Yu. Zorenko, and K. Nejezchleb, Phys. Status Solidi B **242**, R119 (2005).
[18] M. Nikl, Phys. Status Solidi A **202**, 201 (2005).
[19] Yu. Zorenko, V. Gorbenko, I. Konstankevych, A. Voloshinovskii, G. Stryganyuk, V. Mikhailin, V. Kolobanov, and D. Spassky, J. Lumin. **114**, 85 (2005).
[20] M. Nikl, A. Novoselov, E. Mihokova, K. Polak, M. Dusek, B. McClune, A. Yoshikawa, and T. Fukuda, J. Phys.: Condens. Matter **17**, 3367 (2005).
[21] Yu. Zorenko, Opt. Spectrosc. **88**, 611 (2000) (in Russian).
[22] Y.-N. Xu and W. Y. Ching, Phys. Rev. B **61**, 1817 (2000).
[23] V. Babin, K. Blazek, A. Krasnikov, K. Nejezchleb, M. Nikl, T. Savikhina, and S. Zazubovich, Phys. Status Solidi C **2**, 97 (2005).
[24] G. Shirinyan, K. L. Ovanesyan, A. Eganyan, A. G. Petrosyan, C. Pedrini, C. Dujardin, I. Kamenskikh, and N. Guerassimova, Nucl. Instrum. Methods Phys. Res. A **537**, 134 (2005).